www.sciencemag.org/content/347/6228/1367/suppl/DC1

Supplementary Materials for

An RNA biosensor for imaging the first round of translation from single cells to living animals

James M. Halstead, Timothée Lionnet, Johannes H. Wilbertz, Frank Wippich, Anne Ephrussi,* Robert H. Singer,* Jeffrey A. Chao*

*Corresponding author. E-mail: ephrussi@embl.de (A.E.); robert.singer@einstein.yu.edu (R.H.S.); jeffrey.chao@fmi.ch (J.A.C.)

Published 20 March 2015, *Science* **347**, 1367 (2015)
DOI: 10.1126/science.aaa3380

This PDF file includes:

Other Supporting Online Material for this manuscript includes the following:
(available at www.sciencemag.org/content/347/6228/1367/suppl/DC1)

Materials and Methods

Construction of TRICK translation biosensors.

PP7 stem-loops that could be translated by the ribosome were generated by gene synthesis by removing potential stop codons in all three reading frames (Genscript). The cassette (405nts) contained six copies of the PP7 stem-loops that were positioned 40 nucleotides apart. The spacing was optimized to prevent ribosomes from potentially stalling at adjacent stem-loops. Shorter distances between stem-loops resulted in significantly reduced levels of protein. The PP7 stem-loops were also optimized for codon usage (tRNA abundance and coding potential) and RNA-folding (mfold) (*28*). The 6x PP7stem-loop cassette was multimerized using SalI and XhoI to generate a cassette with 12 copies of the PP7 stem-loops.

The PP7 stem-loop cassette was then inserted into a modified version of the pmaxGFP plasmid (Lonza), which uses the cytomegalovirus (CMV) immediate early promoter for expression and contains the β-globin-IgG chimeric intron in the 5′ UTR. The GFP sequence was replaced by the fluoregen activating protein dNP799 that also contained an N-terminal NLS with three copies of the hemagglutinin (HA) – tag (*29*). The PP7 stem-loop cassette was fused in-frame with the C-terminus of dNP799. After the stop codon, the 24x MS2 stem-loop cassette was placed. The final construct was therefore CMV promoter - chimeric intron – NLS - 3xHA – dNP799 – 6x (12x) PP7 stem-loops – stop codon – 24x MS2 stem-loops – SV40 polyA. In order to induce expression of the reporter mRNA, the CMV promoter was replaced by 45 copies of the E/GRE recognition elements that are bound by a heterodimer of retinoid-X-receptor (RXR) and a synthetic ecodysone receptor (VgEcR) and can activate transcription in the presence of ponasterone A (*30, 31*). The 5′ TOP TRICK reporter mRNA was generated by cloning the Tetracycline-inducible promoter and 5′ UTR of human RPL32 from rpL32-β-globin in front of a construct that contained the chimeric intron – Renillia luciferase – 12xPP7 stem-loops – stop codon -24xMS2 stem-loops – SV40 polyA (*19*).

Fluorescent protein plasmids.

Chimeric fusions of the PP7 coat protein (PCP) and MS2 coat protein (MCP) with fluorescent proteins were generated in order to label reporter mRNAs. An NLS was added to PCP and this was fused to the N-terminus of EGFP to make NLS-PCP-EGFP. A single chain tandem dimer of MCP, which also contained and NLS, was fused to the N-terminus of TagRFP-T resulting in NLS-2xMCP-TagRPF-T. The use of the tdMCP allowed lower concentrations of the fluorescent fusion protein to be used in imaging experiments without affecting RNA-binding as previously reported (*32*). Both fluorescent fusion proteins were cloned into the pHAGE-UbiC lentiviral vector, which uses the human ubiquitin C promoter to drive expression (*33*). In order to improve imaging in the red channel, TagRFP-T was replaced with the Halo protein that allowed labeling with Janelia Fluor 549 (*34*).

Cell lines.

U-2 OS

NLS-PCP-GFP and NLS-MCP-RFP were stably expressed in the human osteosarcoma U-2 OS cell line by lentiviral transduction using standard protocols. Cells expressing both fluorescent fusion proteins at levels appropriate for single-molecule imaging experiments were isolated by fluorescence-activated cell sorting. After enriching for double-positive cells, individual clones were isolated and tested in imaging experiments. The ponasteroneA-inducible U-2 OS cell line was generated by stable integration of the pERV3 plasmid, which contains an expression cassette for the VgEcR and RXR receptors, by G418 selection (Agilent) (*31*). Inducible expression of luciferase from the pEGSH-Luc plasmid was used to identify clones that demonstrated robust ponasteroneA induction. U-2 OS cell lines were cultured in DMEM (Life Technologies) supplemented with 10% FBS (Sigma) and 1% Pen Strep (Life Technologies).

HeLa

NLS-PCP-GFP and NLS-MCP-Halo were stably expressed in the human HeLa cell line by lentiviral transduction using standard protocols. The HeLa cell line contained the rtTA2-M2 tetracycline reverse transactivator for doxycycline inducible expression and a single FLP recombinase-mediated cassette exchange (RCME) site that allowed stable integration of TRICK reporter mRNAs into a defined silent but activatable locus (*35*). RMCE of TRICK reporter mRNAs was performed by replacement of the hygromycin-thymidine kinase (*hygtk)* positive-negative selection cassette. Cells were transfected with 2μg of the targeting plasmid with 2μg of pCAGGS-FLPe-IRESpuro using Lipofectamine 2000 (Life Techonologies) according to the manufacturer's protocol. Single hygromycin-resistant colonies were picked and selected for their luciferase expression. HeLa cell lines were cultured in DMEM supplemented with Tet-free FBS (Clonetech) and 1%Pen Strep. In order to visualize P-bodies in cells, a DDX6-Turquoise2 fusion protein was cloned into the pHAGE UbiC lentiviral vector and was stably integrated. Cells expressing NLS-PCP-GFP, NLS-MCP-Halo and DDX6-Turquoise2 were isolated by FACS.

Western blotting.

U-2 OS cells cultured in 10cm dishes were washed in ice-cold 1xPBS and lysed on ice by the addition of lysis buffer (50mM Tris-HCl (pH7.4), 150mM NaCl, 1mM EDTA, 1%(v/v) NP-40) supplemented with one Complete mini EDTA-free protease inhibitor tablet (Roche). Cells were collected by cell scraping and incubated on ice for 5 minutes prior to centrifugation at 15,000*g* for 20 minutes at 4°C. The supernatant (5μg) was resolved by SDS-PAGE and transferred to nitrocellulose membrane (Life Technologies). Non-specific interactions were blocked by incubating the membrane in 1xPBS supplemented with 5%(w/v) non-fat dry milk (Bio-Rad) and 0.05%(v/v) Tween 20 (Sigma) for 1 hour at room temperature. Membranes were probed with an anti-HA high affinity antibody (Roche 3F10, 1:1000 dilution) and β-actin (Sigma A1978, 1:2000 dilution) in 1xPBS supplemented with 1% BSA (Sigma) and 0.05% (v/v) Tween 20 for 1 hour at room temperature. Membranes were washed three times with 1xPBS with 0.05%(v/v) Tween 20 and incubated with IRDye 680 and IRDye 800 (Li-Cor, 1:10,000 dilution) for 30 minutes at room temperature. Membranes were imaged using an Odyssey infrared imaging system (Li-Cor) and quantitative densitometry was performed using ImageJ software (US National Institutes of Health).

Polysome analysis

HEK293T cells were transfected with NLS-MCP-RFP, NLS-PCP-GFP and a TRICK reporter mRNA using Lipofectamine 2000 (Life Techonologies) two days prior to harvesting the cells. Cells were washed with ice cold 1xPBS supplemented with 100 μg ml^{-1} cycloheximide and collected by cell scraping on ice followed by centrifugation at 500*g* for 10 minutes at 4°C. Cell pellets were lysed in 10mM HEPES pH 7.4, 5mM $MgCl_2$, 150mM KCl, 1mM DTT, 2% NP-40, 20U ml^{-1} SUPERase In (Life Technologies), 100 μg ml^{-1} cycloheximide and Complete EDTA-free protease inhibitor (Roche). After incubation on ice for 5 minutes, cell debris was removed by centrifugation at 13,000*g* for 10 minutes at 4°C. Lysates were loaded onto at 10% to 50% linear sucrose gradient (10mM HEPES pH 7.4, 5mM $MgCl_2$, 150mM KCl, 1mM DTT and 100 μg ml^{-1} cycloheximide) and centrifuged in a Beckman SW40 rotor at 35,000rpm for 3 hours. After centrifugation, sucrose gradients were fractionated and absorbance (254nm) was continuously recorded. Fractions (1ml) were collected and TCA precipitated before Western blot analysis. Membranes were probed for NLS-MCP-RFP (MS2 coat protein antibody, Millipore) and NLS-PCP-GFP (GFP antibody, Roche).

RNA FISH and immunofluorescence.

MS2 RNA FISH – GFP-booster IF

U-2 OS cells were cultured on coverslips in DMEM (Life Technologies) supplemented with 10% FBS (Sigma) and 1% Pen Strep (Life Technologies) and washed with 1xPBS before fixation with 4% paraformaldehyde (Electron Microscopy Sciences) in PBSM (1xPBS with 5mM $MgCl_2$) for 20 minutes at room temperature. Cells were washed two times with PBSM and permeabilized with 0.5% (v/v) Triton X-100 (Sigma) in PBSM for five minutes at room temperature. After permeabilization, cells were washed two times with PBSM and then incubated with prehybridization solution (2xSCC, 10% (v/v) formamide (Sigma)) for five minutes at room temperature. Cells were then hybridized with 250nM of MS2 RNA FISH probes (Biosearch Technologies) in 2xSSC, 10% (v/v) formamide (Sigma), 10% (w/v) dextran sulfate for four hours at 37°C. Following hybridization, cells were washed with prehybridization solution for 30 minutes at 37°C. In order to prepare cells for immunofluorescence, after the prehybridization wash, cells were washed two times with PBSMT (PBSM with 0.1% (v/v) Tween 20) and then blocked with 4% (w/v) BSA in PBSMT for 10 minutes at room temperature. Cells were then incubated with 50 ng ml^{-1} of GFP-Booster (Chromotek) in blocking buffer for one hour at room temperature. Cells were washed three times with PBSMT for five minutes at room temperature before counterstaining DNA with DAPI (0.5 mg l^{-1}) and mounted on slides using ProLong gold reagent (Life Technologies).

RNA FISH – SG and P-body IF

HeLa cells were cultured on coverslips in DMEM (Life Technologies) supplemented with 10% Tet-free FBS (Clonetech) and 1% Pen Strep (Life Technologies) and washed with 1xPBS before fixation with 4% paraformaldehyde (Electron Microscopy Sciences) for 20 minutes at room temperature. Cells were washed two times with PBSM and permeabilized with 0.5% (v/v) Triton X-100 (Sigma) in PBSM for five minutes at room temperature. After permeabilization, cells were washed two times with PBSM and then

incubated with prehybridization solution (2xSCC, 10% (v/v) formamide (Sigma)) for five minutes at room temperature. Cells were then hybridized to 250nM of Renilla mRNA FISH probes (Quasar570, Biosearch Technologies), DDX6 antibody (3.3µg ml^{-1}, Bethyl labs), TIAR antibody (2.5µg ml^{-1}, BD) in 2xSSC, 10% (v/v) formamide (Sigma), 10% (w/v) dextran sulfate, 0.5% BSA for three hours at 37°C. Following hybridization, cells were washed with prehybridization solution for 30 minutes at 37°C containing 2° antibodies (goat anti-rabbit Alexa647, donkey anti-mouse Alexa488, Life Technologies). Cells were washed for a second time in prehybridization solution without 2° antibodies at room temperature for 30 min. Cells were washed three times with PBSMT for five minutes at room temperature before counterstaining DNA with DAPI (0.5 mg l^{-1}) and mounted on slides using ProLong gold reagent (Life Technologies).

Image acquisition.

Live cell.

U-2 OS cell lines expressing NLS-PCP-GFP and NLS-MCP-RFP (~10,000 cells) were seeded on a 0.17mm delta T dish (Bioptechs) and cultured in DMEM, 10% (v/v) FBS and 1% (v/v) Pen Strep. The following day, cells were transfected with 0.5-1µg of plasmids expressing reporter mRNAs using FuGENE 6 (Roche). Two days after transfection, cells were washed with Hank's Balanced Salt Solution (HBSS, Life Technologies) and placed in L-15 media supplemented with 10% (v/v) FBS for imaging. For ponasteroneA induction experiments, the drug was added to cells either 30 minutes or two hours prior to imaging.

Cells were imaged on a custom built wide-field microscope based an Olympus IX-71 inverted microscope using an 150x, 1.45NA UApo oil immersion objective (Olympus) equipped with two precisely aligned back-illuminated EMCCD cameras (Andor iXon DU-897). A 488nm Argon laser ion (Melles Griot) and a 561nm solid-state diode laser (Cobolt) were used as excitation sources. The lasers were combined into an optical fiber and reflected towards the objective by a multiline dichroic mirror (Chroma). Fluorescence was collected by the same objective lens and a dichroic mirror was used to split the fluorescence into to the two EMCCD cameras. Cells were maintained at a constant temperature of 37°C using a heated lid and objective heater (Bioptechs) and allowed to equilibrate for at least one hour prior to imaging.

Images were acquired using MetaMorph (Molecular Devices) as single planes at frame rates of 20Hz (50ms exposure) – 66Hz (15ms exposure). For rapid imaging (66Hz), only the center quadrant of the chip (256x256 pixels) on both cameras was used for imaging. Short exposure times allowed single mRNAs to be tracked in two channels (green and red) simultaneously for at least 200 frames.

HeLa cells lines expressing NLS-PCP-GFP, NLS-MCP-Halo, DDX6-Turquoise2 (~10,000 cells) and TRICK reporter mRNAs were seeded on a 35mm µ-Dish (Ibidi) and cultured in DMEM, 10% (v/v) Tet-free FBS and 1% (v/v) Pen Strep two days before imaging. Expression of TRICK reporter mRNAs was induced by addition of 1µg ml^{-1} doxycycline for one hour prior to imaging. For stress experiments, arsenite (0.5mM) was also added to media following doxycycline induction prior to imaging. Cells were relieved from stress by washing five times with 2mls of media without arsenite.

Cells were imaged on a spinning-disk confocal microscope based on an Olympus IX81 inverted microscope equipped with a Yokogawa CSU-X1 scanhead with Borealis modification (Andor) using a 100x 1.45NA PlanApo TIRFM oil immersion objective (Olympus). Images were collected on two precisely aligned back-illuminated EMCCD cameras (EvolveDelta, Photometrics). Solid-state lasers (445nm, 491nm, 561 nm; Cobolt) were used as excitation sources. Cells were maintained at a constant temperature of 37°C and 5% CO_2 within an incubation box. Images were acquired using Visiview (Visitron) as single planes at frame rates of 20Hz (50ms exposure).

For fluorescence recovery after photobleaching (FRAP) experiments of TRICK reporter mRNAs within P-bodies, cells were induced for 1 hour with doxycycline (1μg ml^{-1}) followed by addition of arsenite (0.5mM). Cells were imaged with NLS-MCP-Halo and an ROI that contained immobile mRNAs clustered was defined. These RNA structures were specifically photobleached using 405nm laser excitation (Cobolt) coupled to a VisiFRAP module (Visitron). Prebleach, bleach and post-bleach images were collected at a frame rate of 0.2Hz for a total of 10 minutes. FRAP recovery curves were generated by calculating the intensity of the ROI from background subtracted images that were normalized for photobleaching.

Fixed cell.

For combined RNA FISH and GFP-booster immunofluorescence experiments, slides were imaged on an Olympus BX-61 upright microscope using a 100x 1.4NA UPlanApo oil immersion objective (Olympus) and Coolsnap HQ camera (Photometrics). An X-cite 120 PC (EXFO) light source was used for illumination with filter sets 31000(DAPI), 41001 (GFP,Atto488) and SP-102v1 (Cy3)(Chroma Technology). Images were acquired with MetaMorph (Molecular Devices) as z-stacks (4μm range in 0.2μm steps).

For combined RNA FISH and SG P-body immunofluorescence experiments, slides were imaged on a Zeiss Axioimager Z1 microscope using a 100x 1.4NA Plan-APOCHROMAT oil immersion objective (Zeiss) and AxioCam MRm camera (Zeiss). An X-cite 120 (EXFO) light source was used for illumination with filter sets for DAPI, Alexa488, Cy3 and Cy5 (Zeiss). Images were acquired with Zen software (Zeiss) as z-stacks (5μm range in 0.24μm steps).

Image analysis.

Live cell – Nuclear mRNA tracking.

Single particle tracking and analysis of mRNAs in two channels was performed in three steps: spot detection, automated tracking, analysis of isolated and co-localized trajectories. Spot detection was performed using custom programs written in Matlab (Mathworks) (*33*). All analysis was performed on unprocessed data. The position of diffraction-limited fluorescent signals arising from single mRNAs was first approximated by applying a spatial bandpass filter to the image and identifying pixels that were above a threshold, which was adjusted for each dataset depending upon the signal-to-noise. Spot candidates were defined as the local maxima within a two-pixel radius. The intensity and position of each spot was calculated to subdiffraction precision by applying a local

background correction and fitting each spot intensity profile to a two-dimensional Gaussian distribution.

Tracking of the mRNAs was performed in a custom program written in IDL (Exelis) (*3*). Trajectories for individual mRNAs were generated from the spots detected in successive frames in time-lapse movies. The number of successive frames an RNA had to be detected in (10), the number of pixels an RNA could move between frames (3) and number of frames an mRNA could disappear in before reappearing (1) was optimized to allow tracking of single mRNA particles.

Tracking was performed in both color channels separately and the two resulting datasets were then compared to identify colocalized particles. A trajectory from the green channel was defined as colocalized with a red channel trajectory when more than 3 datapoints from the green trajectory were found within 3 pixels of their counterparts from the red trajectory. As an extra stringency criterion, we enforced that the average distance between all codetected spots of two colocalized trajectories was below a threshold of 4 pixels (428nm). After running this colocalization algorithm once, we measured the average position offset between colocalized red and green data points and used it to register the two tracking datasets with subpixel precision. The colocalization algorithm was then run a second time on the registered sets of trajectories. Since we used stringent criteria to define trajectories in each channel, we ran the risk of underestimating the colocalization fraction. To solve this issue, we included an extra step in which we looked for matches between trajectories from one channel and isolated spots (i.e. non part of any trajectory) in the other channels. To define a trajectory colocalized with isolated spots, we ensured that it colocalized with a statistically significant number of spots in the other channel. The distance threshold used was the same as that used for trajectory matching, and the minimum number of co-detections for statistical significance was defined 2 standard deviations away from the average expected number of codetection ($p<0.05$ for Poisson statistics). The expected number of false codetections was calculated based on the number of frames in the trajectory, and the expected number of false detections per frame. For each frame, the false positive rate was computed using the total number of spots detected in the other channel at each frame, the total area of the image and the distance threshold for colocalization; false positive spots were assumed to occur randomly in space.

Following colocalization, we performed the diffusion analysis separately on the two datasets corresponding respectively to the colocalized and isolated (i.e. for which no match was found in the other channel) trajectories. All data presented in the article corresponds to the NLS-MCP-RFP signal (located at the 3′ UTR of our mRNA construct). All the diffusion analysis results presented in this work were based on trajectories separated using the stringent colocalization criterion (only trajectories matched to bona fide trajectories were included; results were unchanged when we included trajectories matched to isolated spots). For each dataset, we assembled the cumulative histogram of the displacement between positions four frames apart (0.060 s). The histogram was fit to either a single diffusing population $P(x) = 1 - \exp(-\frac{x^2}{4Dt})$, or a 2-state model in which particles can occupy two states, each with a distinct diffusion coefficient: $P(x) = 1 - A\exp\left(-\frac{x^2}{4D_1 t}\right) - (1-A)\exp(-\frac{x^2}{4D_2 t})$ (fig. S10)

Live cell – Cytoplasmic mRNA tracking during stress

The tracking of dual colored single mRNA molecules was performed for each green and red channel individually and consisted of four steps: (1) Segmentation of the cells in a nuclear and cytoplasmic region of interest (ROI), (2) Single particle detection in every frame, (3) joining of detected particles to trajectories, and (4) co-localization of trajectories from both channels in order to determine the translation state of the respective mRNA particle.

Image segmentation, spot detection and tracking were performed by the NIS-Elements AR software package (Nikon). The nucleus and the cell borders were determined by thresholding and defined as binary layers and subtracted from each other, which yielded the cytoplasmic ROI relevant for spot detection and tracking.
The program used circularity, the typical spot diameter, and the contrast a spot as parameters for their detection. Here, a fixed spot diameter of 0.38 μm was chosen, while the contrast heavily depended on the channel and cell state during an imaging session (no stress/stress/relief from stress). It was therefore necessary to optimize spot detection per cell and imaging frame.

Next, spots were joined to trajectories based on their location in subsequent frames. The center of a spot was defined as its maximum intensity and random motion was assumed. The maximum spot speed was set to 6 $\mu m\ s^{-1}$ which defined an area around the spot in which the next spot was likely to be found. Based on the movement model and speed, a trajectory was terminated when no spot was within 1.8 standard deviations of its predicted position. Backward tracking and a maximum detection gap size of 1 frame were allowed.

After the connection of spots to trajectories, it was checked whether two trajectories could be connected. This was allowed when the gap size between the trajectories was not larger than 1 frame and the predicted position of the second trajectory was within 1.5 standard deviations of the previous trajectory. Joined spot trajectories were then individually checked for accuracy.

As a last step, co-localization analysis for all tracks of both channels was performed using the custom Matlab (Mathworks) script described in the nuclear mRNA tracking section. Colocalization criteria had to be adjusted to reflect the different signal-to-noise of the dataset; namely, two trajectories were considered to be co-localized when at least two spots of the green trajectory were within 1 pixels (92nm) in x,y of the red trajectory. Co-localization was then checked for accuracy by evaluating individual tracks.

Fixed cell.

Three-dimensional image stacks were maximally projected on a single two-dimensional plane for analysis of RNA spatial distributions. Nuclei were automatically segmented on the Maximum Intensity Projection of the DAPI z-stack using a custom Matlab program. Spots for all mRNAs (FISH) and untranslated mRNAs

(immunofluorescence) were detected and their position measured using the program described above (Nuclear mRNA Tracking). Cell boundaries were manually outlined on the Maximum Intensity Projection of the FISH z-stack using ImageJ (Rasband, W.S., ImageJ, U. S. National Institutes of Health, Bethesda, Maryland, USA, http://imagej.nih.gov/ij/, 1997-2012.). The minimum distance of each spot to the segmented nucleus was determined using a custom Matlab script.

Colocalization of mRNAs with P-bodies in fixed cells

The quantification of mRNA colocalization with P-bodies was performed on maximum intensity projected images of fixed single cells. The analysis process could be divided into three parts: (1) Quantification of total mRNA particles (labeled by FISH) in the cell, (2) definition of binary masks for both the DAPI channel (nucleus) and P-bodies, and (3) quantification of all mRNA spots that colocalize with P-bodies.

The initial whole cell mRNA counting was performed on the single-molecule FISH data. The procedure was based on Gaussian distribution fitting and performed by custom scripts written in Matlab as previously described (Mathworks). Nuclei were segmented using the DAPI signal and nuclear mRNAs were excluded from further analysis. P-bodies were segmented based upon DDX6 immunofluorescence and mRNAs that colocalized with these cytoplasmic structures were counted. The mRNA content of clusters that were found in P-bodies was determined by measuring the total intensity and dividing it by the intensity of a single mRNA.

Construction of transgenes and transgenic lines for osk-TRICK reporter assay in Drosophila

A *Bam*HI/*Bgl*II fragment from pSL-6xMS2 (*36*) containing 6xMS2 stem-loops was ligated into a *BamH*I site that was introduced right after the stop codon (*24*) of a 6.5 kb genomic rescuing construct pGem-g-osk (*20*). The multimerized 12xPP7 stem-loop cassette was amplified using PCR primer with *Mlu*I sites overhanging (ATTAACGCGTCAGATCCTACCTGCAAAGCAC, TACGCGTGAAGATCTTGTATCTCTGATGGAC) and ligated in frame into an *Mlu*I site of the p-Gem-g-osk-6xMS2 construct. A *Not*I/*Xho*I fragment from p-Gem-g-osk-6xMS2 containing the *osk* promoter and osk-12xPP7-6xMS2 was inserted into pCasper4. To generate NLS-PCP-GFP and NLS-MCP-RFP, *Not*I/*Acc65I* fragments of either pHAGE-UbiC-NLS-HA-2xPCP-2xEGFP or pHAGE-UbiC-NLS-HA-2xMCP-2xTagRFP-T were cloned into pHsp83 vector (a kind gift from Imre Gáspár).
All transgenes were introduced into the w^{1118} strain by P element-mediated germline transformation.

Preparation of ovaries and Western Blot analysis

Ovaries from well-fed female flies were dissected in 1xPBS, supplemented with 1% Triton X-100 (Sigma) and Complete mini EDTA-free protease inhibitor tablet (Roche). Ovaries were homogenized using a micropestle and incubated for 10 minutes on ice prior to centrifugation at 15,000*g* for 20 minutes at 4°C. Supernatants were denatured by the

addition of sample buffer and boiling for 7 minutes at 95°C, resolved by SDS-PAGE and analyzed by immunoblotting against Oskar (rabbit anti-Oskar) (*37*) and Tubulin (Sigma T5168). w^{1118} flies were used as the wild-type control.

Drosophila immunofluorescence and microscopy analysis
For a comparison of osk-TRICK reporter signals and Oskar protein, ovaries from well-fed female flies (in which only half of the wild-type osk mRNA was present (osk A^{87}/+)), expressing *osk-TRICK* mRNA, NLS-MCP-RFP and NLS-PCP-GFP were dissected and fixed for 20 minutes in 1xPBS, supplemented with 4% paraformaldehyde (Electron Microscopy Sciences). Ovaries were permeabilized for 1 hour in 1x PBS with 1% Triton X-100, then blocked with blocking buffer (1xPBS with 0.5% BSA and 0.1% Triton X-100) for 30 minutes and incubated with rabbit anti-Oskar (*37*) in blocking buffer for 2 hours. After removal of primary antibody, ovaries were incubated with goat anti-rabbit conjugated to Cy5 (Jackson ImmunoResearch 111-175-003) in blocking buffer for 1 hour. Confocal z-stacks for quantification were collected on a Leica TCS SP8 confocal microscope (HC PL APO CS2 63X/1.4 Oil). For quantification of fluorescent signals, the sum of z-stacks was calculated per image and integrated signal intensity of poleplasm area and oocyte area was measured using ImageJ (http://rsb.info.nih.gov/ij/). Images for the overview image were collected on a Zeiss LSM 780 NLO confocal microscope (C-Apochromat 40X/1.20W).

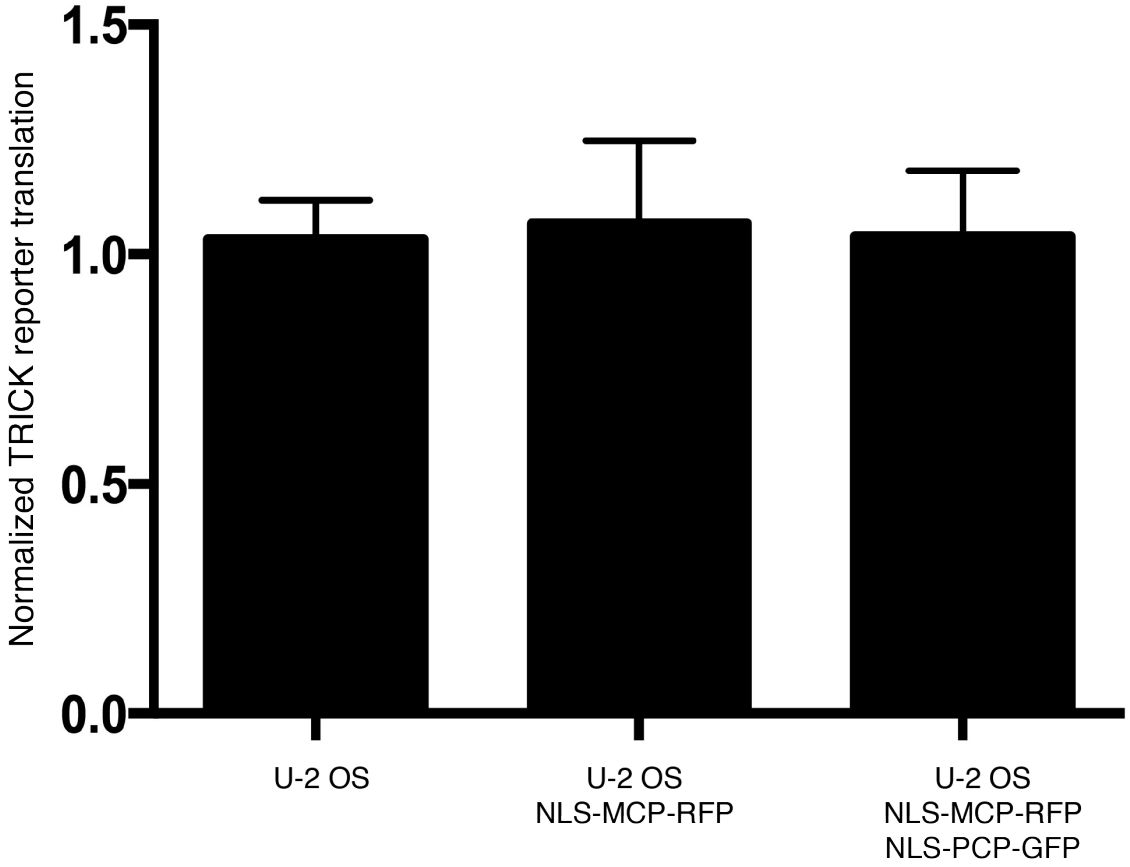

Fig. S1. Translation of TRICK reporter mRNA in U2 OS cells. Quantification of immunoblot of HA-tagged TRICK reporter protein levels normalized to β-actin protein. Error bars indicate s.e.m. (n = 3).

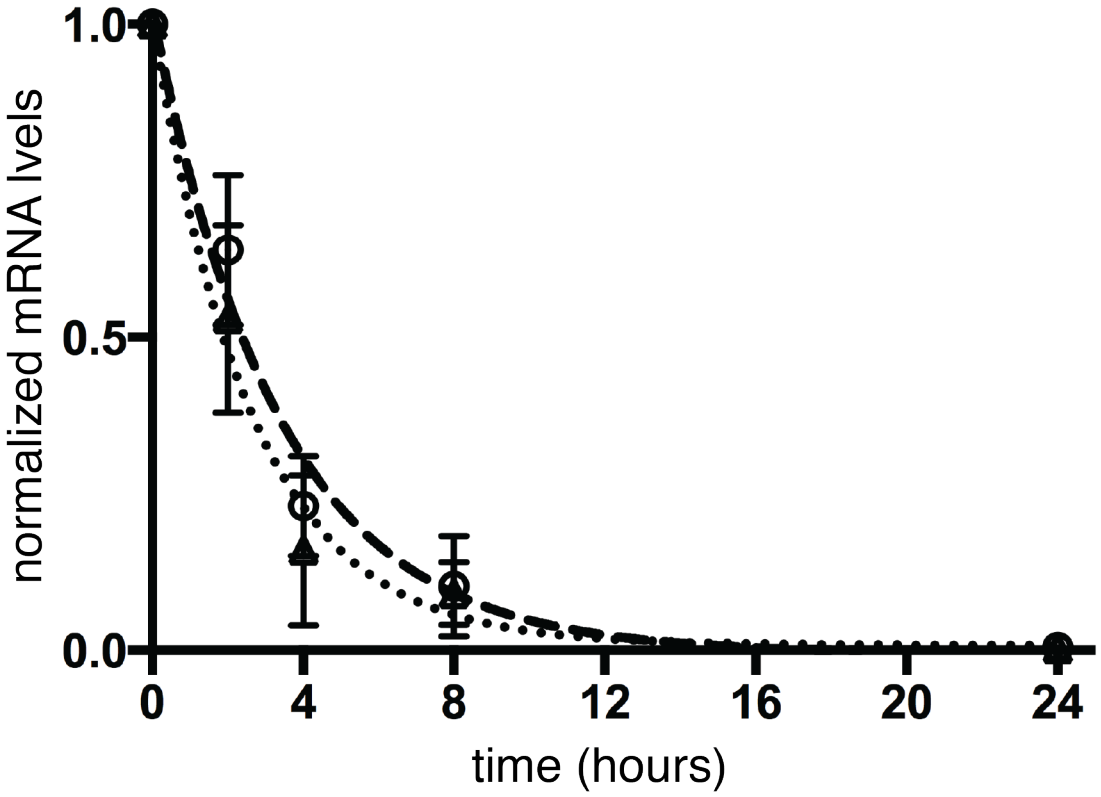

Fig. S2. Binding of fluorescent coat proteins to TRICK reporter mRNA does not alter mRNA decay. (A) The TRICK reporter mRNA was transfected into U-2 OS cells with (····) and without (- - -) NLS-PCP-GFP and NLS-MCP-RFP. Transcription was blocked by addition of ActD and RNA was isolated as a function of time. The levels of TRICK reporter mRNA was determined by RT-qPCR and was normalized to *GAPDH* mRNA. Error bars indicate s.e.m. (n = 3).

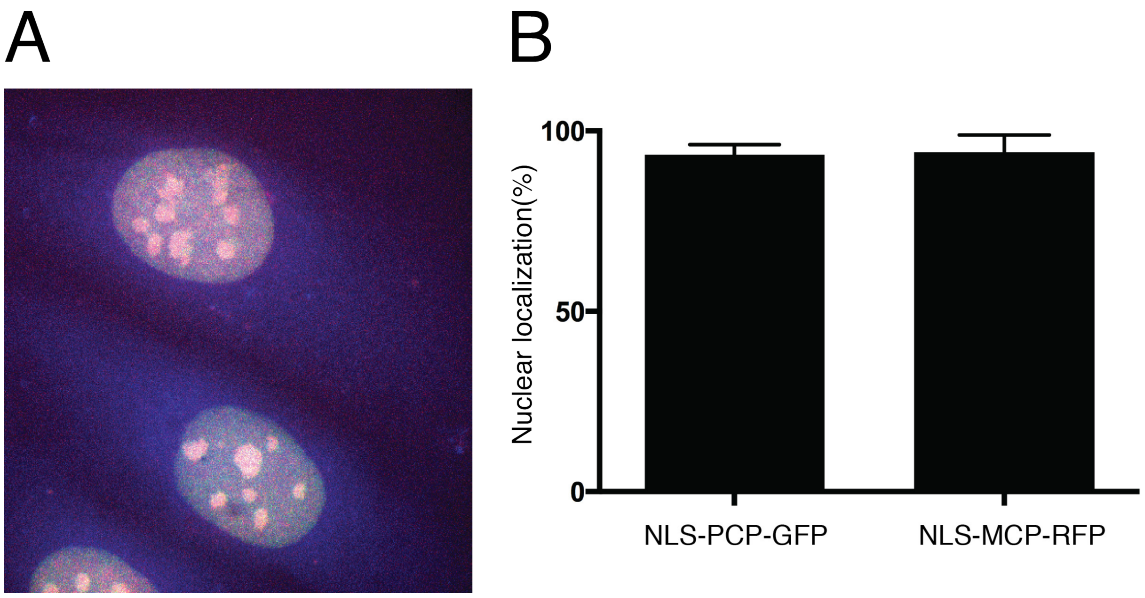

Fig. S3. Fluorescent coat proteins are restricted to the nucleus in the absence of TRICK mRNAs. (A) Representative image of U-2 OS cells expressing NLS-PCP-GFP and NLS-MCP-RFP. (B) Quantification of amount of NLS-PCP-GFP and NLS-MCP-RFP in the nucleus compared to total cellular fluorescence in each channel. Error bars indicate s.e.m. (n = 20 cells).

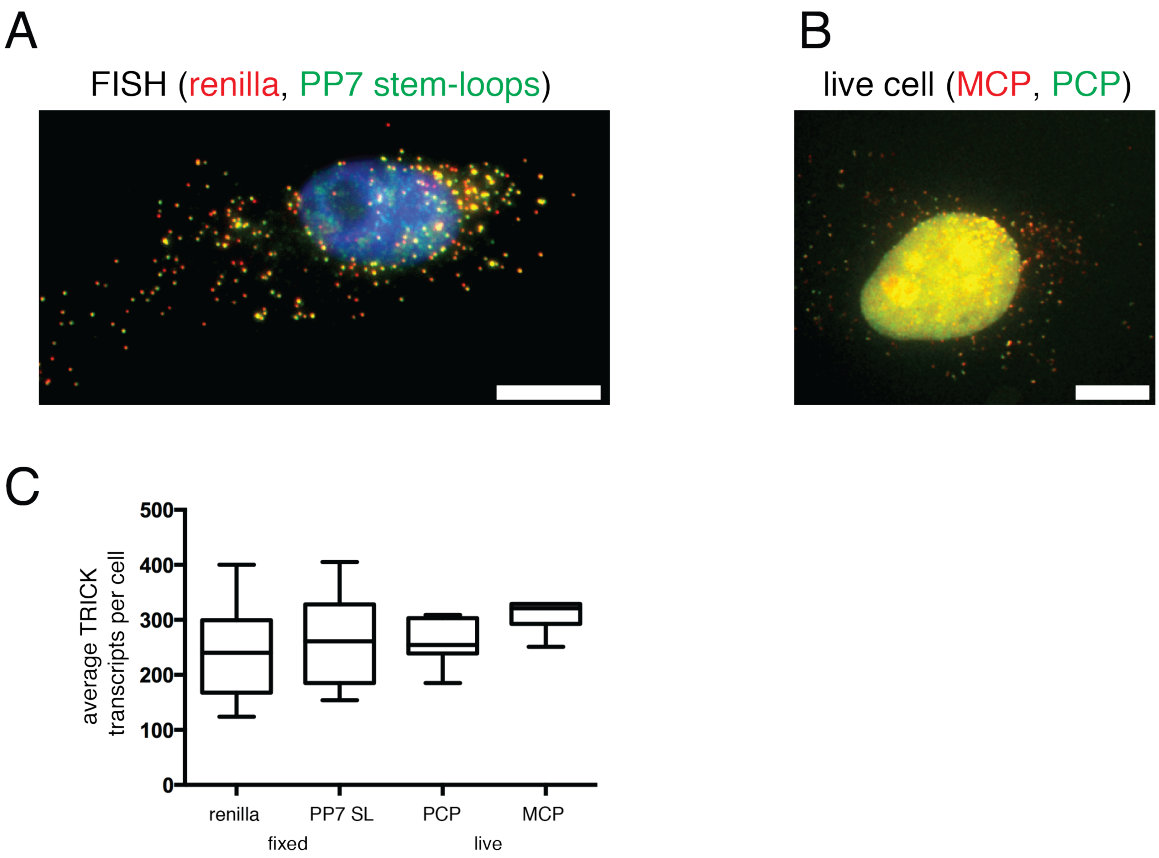

Fig. S4. Single-molecule detection of all TRICK reporter mRNAs in HeLa cells. (A) Representative single-molecule FISH image of HeLa cells expressing TRICK reporter mRNA that were treated with puromycin (100 μg ml^{-1}) for 30 minutes prior to induction (doxycycline 1 μg ml^{-1}) for 60 minutes. FISH probes targeting both the Renilla coding sequence (Quasar570, red) and PP7 stem-loops (Quasar670, green) detect transcripts with nuclei labeled by DAPI (blue). (B) Representative live cell image of HeLa cells expressing TRICK reporter mRNAs that were treated with puromycin (100 μg ml^{-1}) for 30 minutes prior to induction (doxycycline 1 μg ml^{-1}) for 60 minutes. NLS-MCP-Halo and NLS-PCP-GFP detects single mRNAs. (C) Quantification of TRICK mRNAs detected by fixed and live cell measurements. Similar average numbers of transcripts were detected by all four measurements (p =0.13, ANOVA). Error bars indicate s.e.m. for fixed cells (n=24 cells) and live cells (n=8 cells). Similar results were also obtained using U-2 OS cells.

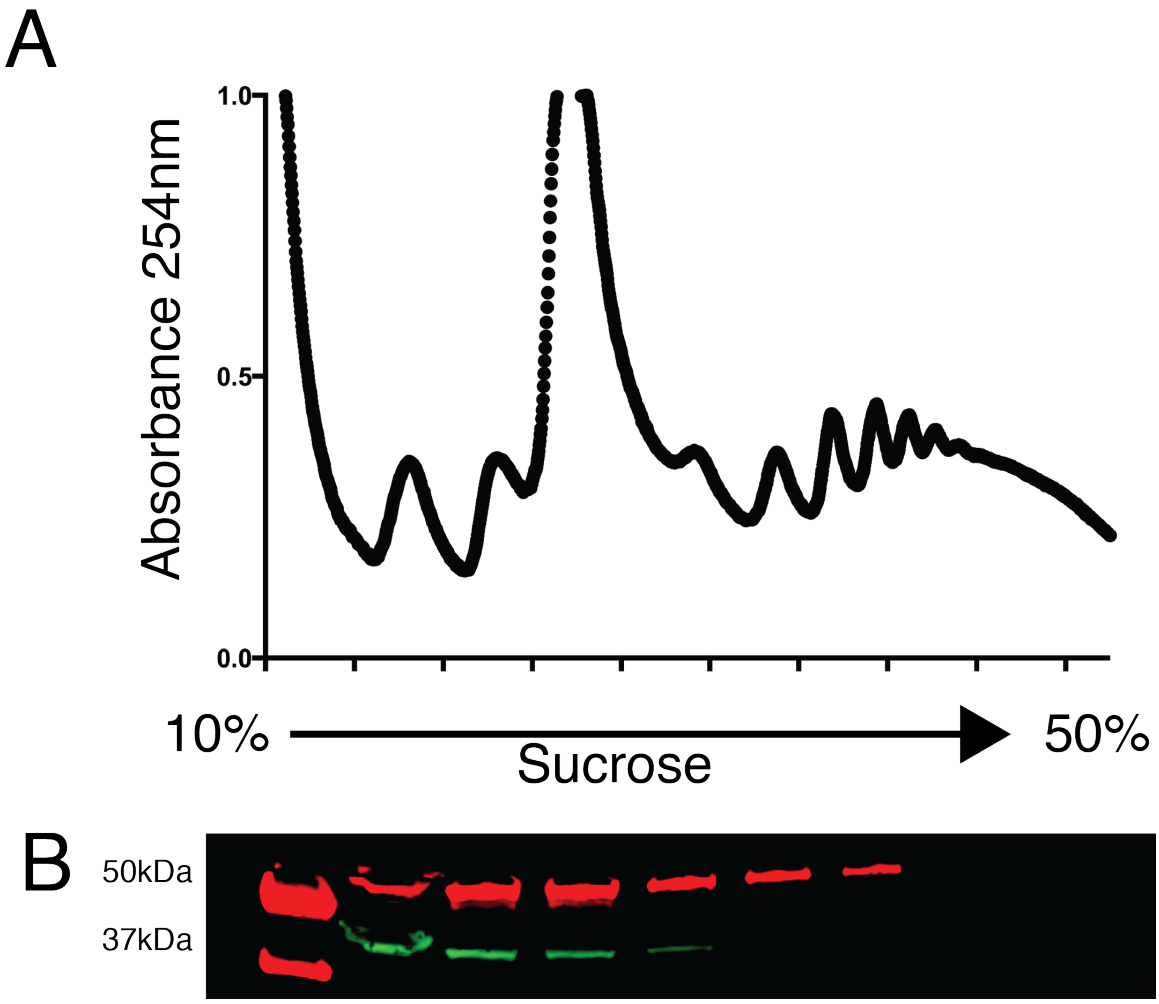

Fig. S5. NLS-PCP-GFP is not associated with polysomes. (A) Polysome profile of HEK293 cells transfected with NLS-PCP-GFP, NLS-MCP-RFP, and TRICK reporter constructs was monitored by absorbance at 254nm. Cell lysates were separated on a 10-50% linear sucrose gradient. (B) Immunoblot of sucrose gradient fractions. NLS-MCP-RFP (red, 56.6kDa) was detected in polysomal fractions, while NLS-PCP-GFP (green, 43.9kDa) was not.

A

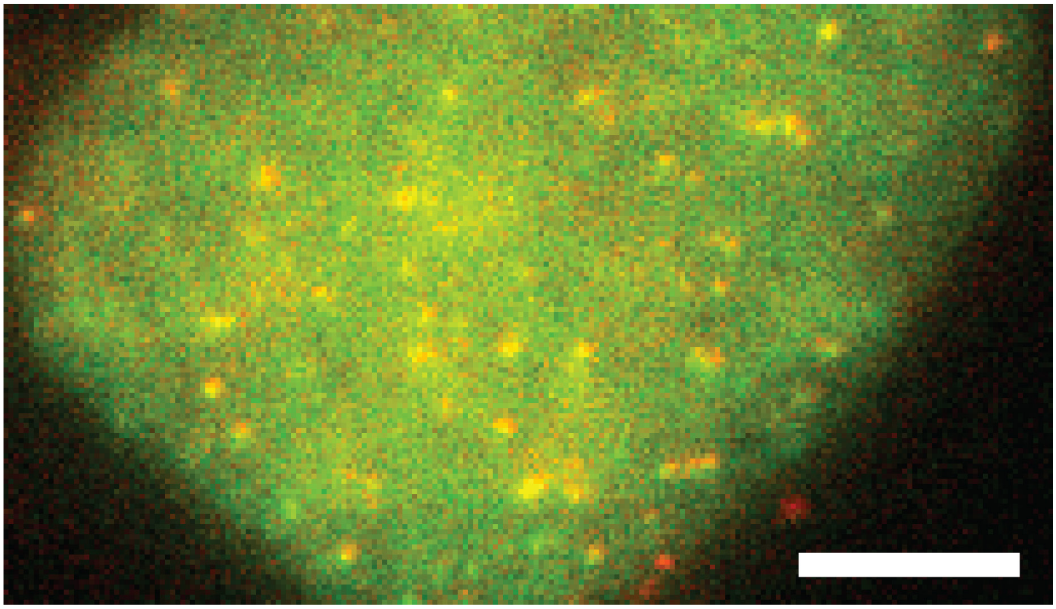

B

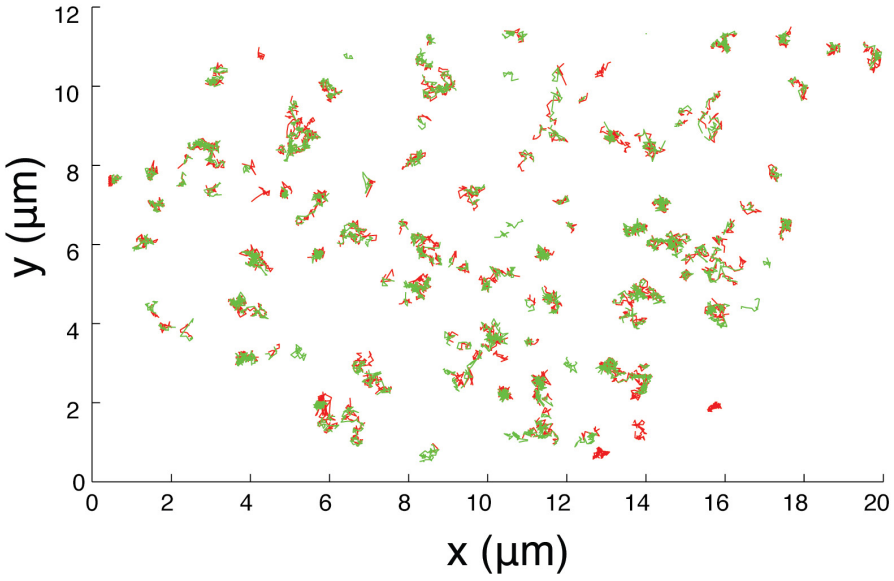

Fig. S6. Tracking of TRICK reporter mRNAs in the nucleus. (A) Representative image of U-2 OS cells expressing TRICK reporter mRNAs 30 minutes after ponA (50µM) induction. (B) Single particle tracking of TRICK reporter mRNAs in nucleus in two channels. Trajectories for mRNAs labeled with NLS-MCP-RFP (red) and NLS-PCP-GFP (green) are shown. The percentage of nuclear mRNAs that co-localize with NLS-MCP-RFP and NLS-PCP-GFP is 91.3± 0.9% (n = 11 cells). Scale bar 2µm.

A

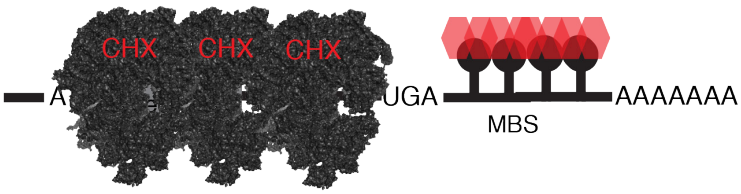

B

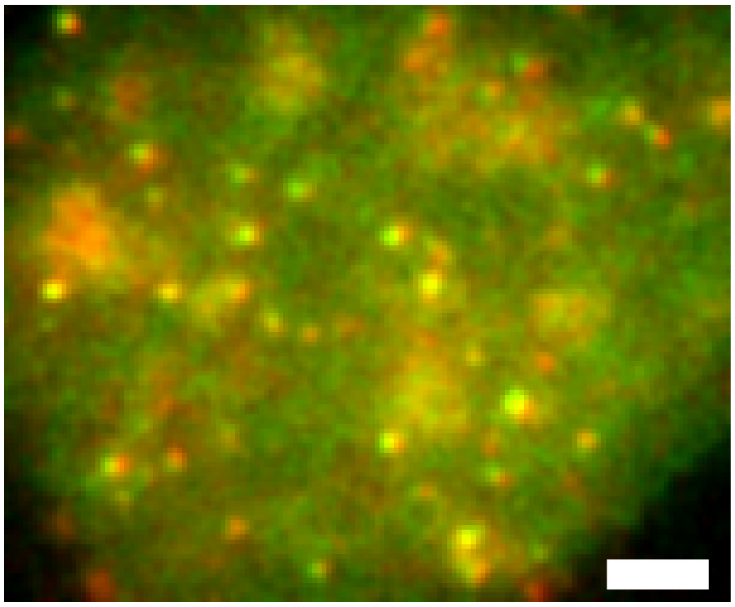

C

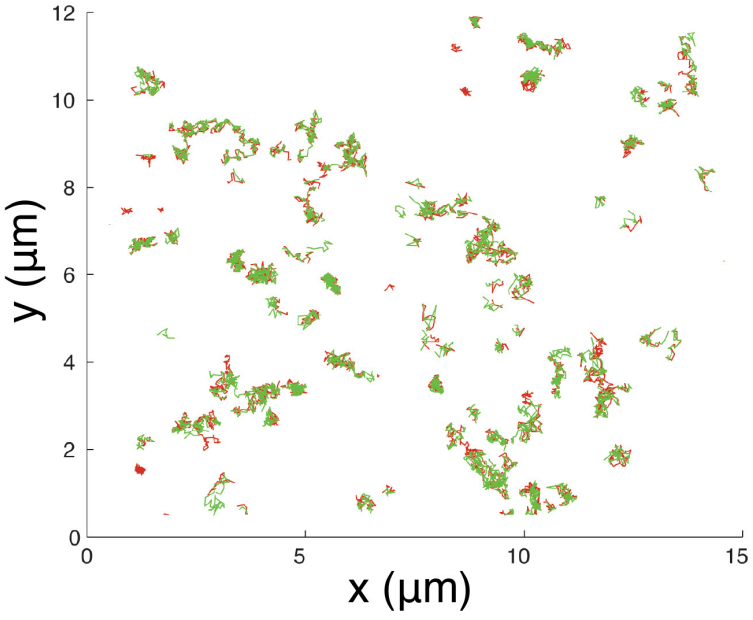

Fig. S7. TRICK reporter mRNAs are not translated in the nucleus. (A) Schematic of TRICK reporter mRNA in the presence of low CHX concentration. Addition of CHX (1μg ml^{-1}) slows down translation and enhances polysome formation, which could prevent NLS-PCP-GFP from binding to the PP7 stem-loops after translation in the nucleus. (B) Representative image of U-2 OS cells expressing TRICK reporter mRNA in the presence of low CHX. (C) Single particle tracking of TRICK reporter mRNAs in nucleus in two channels. Trajectories for mRNAs labeled with NLS-MCP-RFP (red) and NLS-PCP-GFP (green) are shown. The percentage of nuclear mRNAs that co-localize with NLS-MCP-RFP and NLS-PCP-GFP in the presence of low CHX is 90.7± 0.6% (n = 11 cells). Scale bar 2μm.

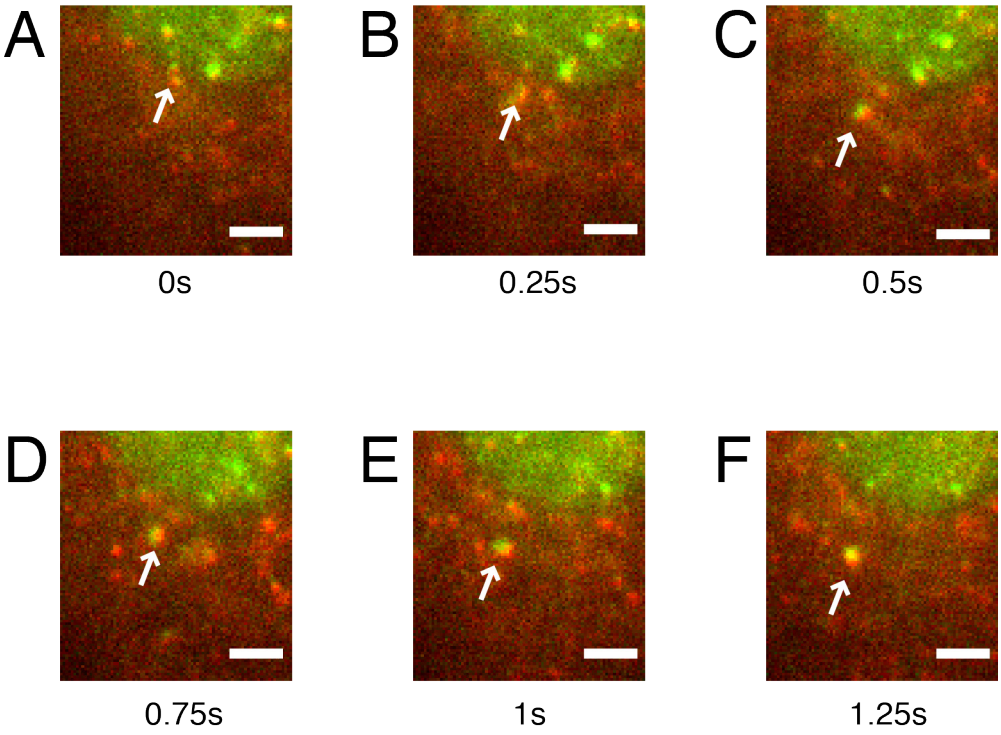

Fig. S8. Export of untranslated mRNAs from the nucleus. (A-F). An mRNA labeled with both NLS-PCP-GFP and NLS-MCP-RFP (shown with arrow) is observed as it is exported from the nucleus and moves into the cytoplasm. Images were acquired with 50ms exposure at frame rate of 4Hz. Scale bar indicates 2μm.

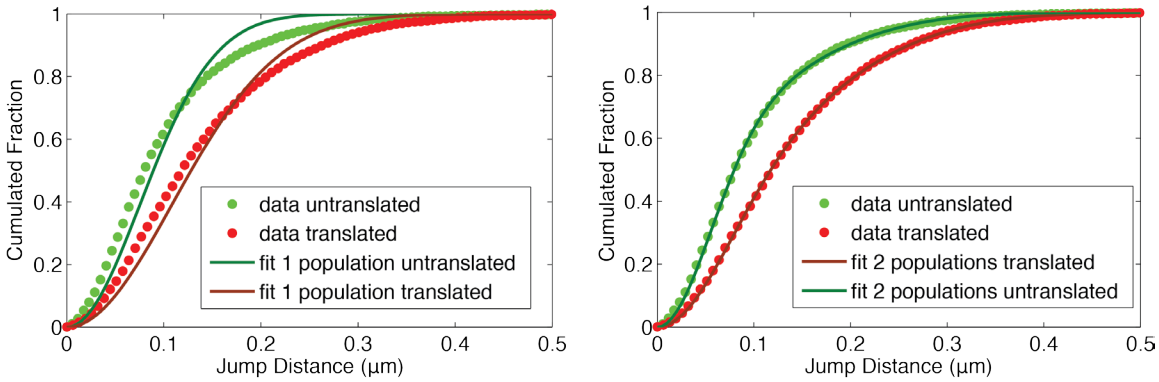

Fig. S9. Diffusional properties of TRICK reporter mRNAs in the cytoplasm. Jump distance histograms over a time lag of 4 frames (60ms) were built from pooled single particle trajectories. Based on automated color colocalization, trajectories were sorted into untranslated species. Untranslated mRNAs correspond to mRNAs detected in both red (NLS-MCP-RFP) and green (NLS-PCP-GFP) channels, whereas RNAs detected in the red channel only were considered translated. Left: A simple model with a single diffusing species poorly fits the data (untranslated: $D = 0.048 \pm 0.003$ µm^2/s; translated: $D = 0.099 \pm 0.004$ µm^2/s). Right: A 2-species model displays a much better agreement. Untranslated species: $D1 = 0.13 \pm 0.005$ µm^2/s, fraction = 36 ± 2%; $D2 = 0.023 \pm 0.001$ µm^2/s, fraction = 64 ± 2%. Translated species: $D1 = 0.17 \pm 0.005$ µm^2/s, fraction = 56 ± 2%; $D2 = 0.039 \pm 0.002$ µm^2/s, fraction = 44 ± 2%. Histograms were built using 3982 jump data points (144 trajectories) for the untranslated species and 7896 data points (557 trajectories) for the translated species.

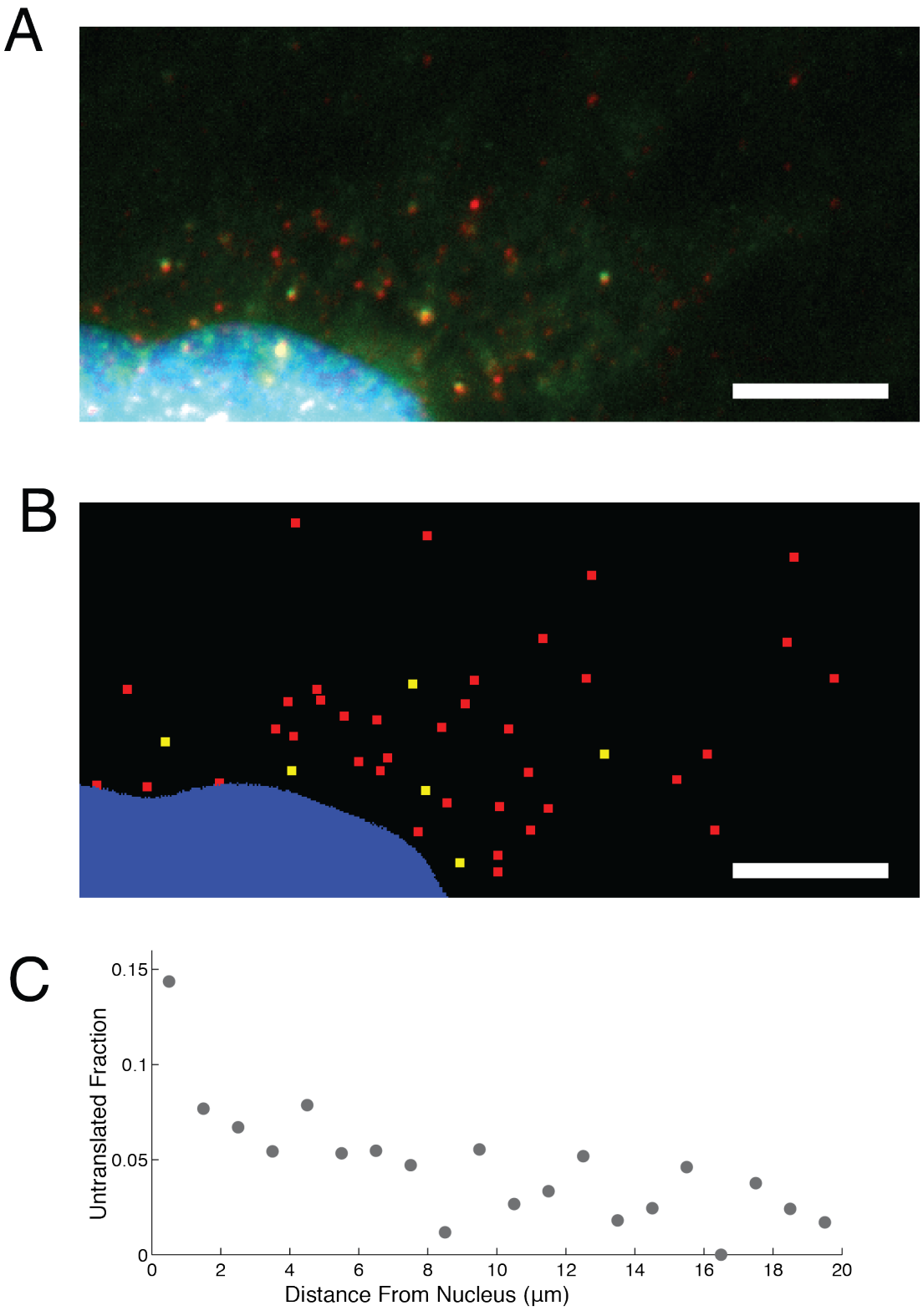

Fig. S10. Spatial distribution of untranslated mRNAs in fixed cells. (A) Representative image of combined IF-FISH in U-2 OS cells. FISH probes targeted for the MS2 stem-loops (red) were used to identify the positions of all mRNAs (red) and

untranslated mRNAs were detected using anti-GFP nanobody (green). The nucleus is stained with DAPI (blue). (B) Spot detection of mRNAs (red) and untranslated mRNAs (green). Scale bar is 5μm. (C) Fraction of untranslated mRNAs as a function of distance from the nucleus.

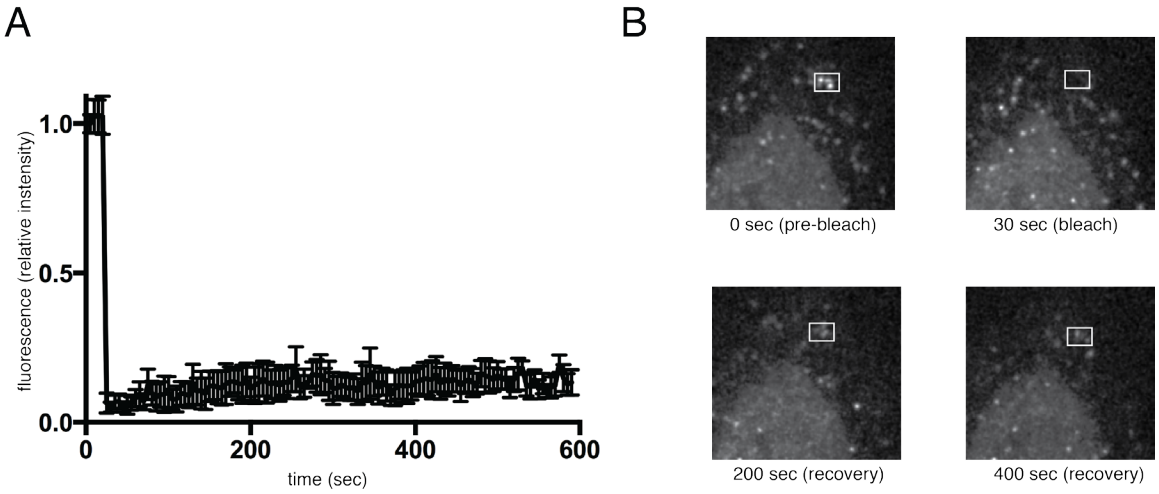

Fig. S11. FRAP of 5′ TOP TRICK mRNAs clustered in P-bodies during arsenite stress. (A) NLS-MCP-Halo FRAP data. Images were collected at a frame rate of 0.2 Hz with three images taken pre-bleach. Error bars indicate s.e.m. for 7 cells. (B) Representative images from FRAP experiment. The fluorescence intensity of clustered mRNAs was found to recover very slowly indicating that these mRNAs were not in rapid exchange with the mRNAs in the cytosol.

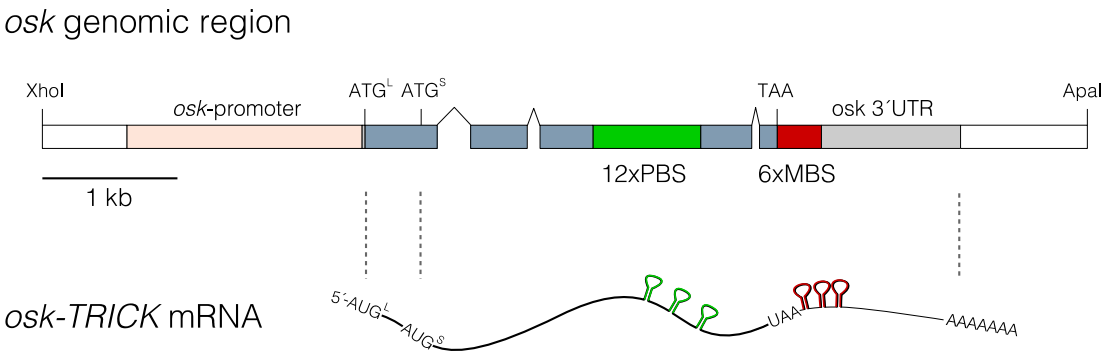

Fig. S12. Schematic of *osk-TRICK* reporter construct.
The positions of 12xPBS and 6xMBS, introduced into the genomic rescuing construct of *osk* and the resulting *osk-TRICK* mRNA are shown.

Movie S1. Diffusion of mRNA molecules in the cytoplasm. mRNAs were simultaneously imaged in both channels (NLS-PCP-GFP, green and NLS-MCP-TagRFP-T, red). Most mRNAs appear as red particles. A few colocalized particles can be observed. Frame rate: 15ms/frame.

Movie S2. Diffusion of mRNA molecules in the cytoplasm in the presence of CHX (100µg ml^{-1}). mRNAs were simultaneously imaged in both channels (NLS-PCP-GFP, green and NLS-MCP-TagRFP-T, red). Most mRNAs appear as colocalized green/red particles. Frame rate: 15ms/frame.

Movie S3. Diffusion of mRNA molecules in the cytoplasm in the presence of Puromycin (100µg ml^{-1}). mRNAs were simultaneously imaged in both channels (NLS-PCP-GFP, green and NLS-MCP-TagRFP-T, red). Most mRNAs appear as colocalized green/red particles. Frame rate: 15ms/frame.

Movie S4. Diffusion of mRNA molecules in the nucleus. mRNAs were simultaneously imaged in both channels (NLS-PCP-GFP, green and NLS-MCP-TagRFP-T, red). Most mRNAs appear as colocalized green/red particles. Frame rate: 15ms/frame.

Movie S5. Diffusion of mRNA molecules in the nucleus in the presence of low CHX (1µg ml^{-1}). mRNAs were simultaneously imaged in both channels (NLS-PCP-GFP, green and NLS-MCP-TagRFP-T, red). Most mRNAs appear as colocalized green/red particles. Frame rate: 15ms/frame.

Movie S6. Movement of mRNAs molecules in the cytoplasm of arsenite (0.5mM) stressed cells. mRNAs were simultaneously imaged in red (NLS-MCP-Halo, Janelia Fluor 549) and green (NLS-PCP-GFP) channels. P-bodies were imaged in cyan (DDX6-Turquoise2) both before and after mRNA imaging to ensure that they did not move during acquisition of mRNA images. Frame rate: 50ms/frame.

Movie S7. Movement of mRNAs molecules in the cytoplasm of cells relieved from arsenite stress. mRNAs were simultaneously imaged in red (NLS-MCP-Halo, Janelia Fluor 549) and green (NLS-PCP-GFP) channels. P-bodies were imaged in cyan (DDX6-Turquoise2) both before and after mRNA imaging to ensure that they did not move during acquisition of mRNA images. Frame rate: 50ms/frame.

References and Notes

1. N. T. Ingolia, S. Ghaemmaghami, J. R. Newman, J. S. Weissman, Genome-wide analysis in vivo of translation with nucleotide resolution using ribosome profiling. *Science* **324**, 218–223 (2009). Medline doi:10.1126/science.1168978

2. B. Schwanhäusser, D. Busse, N. Li, G. Dittmar, J. Schuchhardt, J. Wolf, W. Chen, M. Selbach, Global quantification of mammalian gene expression control. *Nature* **473**, 337–342 (2011). Medline doi:10.1038/nature10098

3. D. R. Larson, D. Zenklusen, B. Wu, J. A. Chao, R. H. Singer, Real-time observation of transcription initiation and elongation on an endogenous yeast gene. *Science* **332**, 475–478 (2011). Medline doi:10.1126/science.1202142

4. A. Raj, A. van Oudenaarden, Single-molecule approaches to stochastic gene expression. *Annu. Rev. Biophys.* **38**, 255–270 (2009). Medline doi:10.1146/annurev.biophys.37.032807.125928

5. J. A. Chao, Y. J. Yoon, R. H. Singer, Imaging Translation in Single Cells Using Fluorescent Microscopy. *Cold Spring Harb. Perspect. Biol.* **4**, a012310 (2012). doi:10.1101/cshperspect.a012310

6. S. Hocine, P. Raymond, D. Zenklusen, J. A. Chao, R. H. Singer, Single-molecule analysis of gene expression using two-color RNA labeling in live yeast. *Nat. Methods* **10**, 119–121 (2013). Medline doi:10.1038/nmeth.2305

7. M. K. Doma, R. Parker, Endonucleolytic cleavage of eukaryotic mRNAs with stalls in translation elongation. *Nature* **440**, 561–564 (2006). Medline doi:10.1038/nature04530

8. D. No, T. P. Yao, R. M. Evans, Ecdysone-inducible gene expression in mammalian cells and transgenic mice. *Proc. Natl. Acad. Sci. U.S.A.* **93**, 3346–3351 (1996). Medline doi:10.1073/pnas.93.8.3346

9. K. Al-Jubran, J. Wen, A. Abdullahi, S. Roy Chaudhury, M. Li, P. Ramanathan, A. Matina, S. De, K. Piechocki, K. N. Rugjee, S. Brogna, Visualization of the joining of ribosomal subunits reveals the presence of 80S ribosomes in the nucleus. *RNA* **19**, 1669–1683 (2013). Medline doi:10.1261/rna.038356.113

10. A. David, B. P. Dolan, H. D. Hickman, J. J. Knowlton, G. Clavarino, P. Pierre, J. R. Bennink, J. W. Yewdell, Nuclear translation visualized by ribosome-bound nascent chain puromycylation. *J. Cell Biol.* **197**, 45–57 (2012). Medline doi:10.1083/jcb.201112145

11. Y. Shav-Tal, X. Darzacq, S. M. Shenoy, D. Fusco, S. M. Janicki, D. L. Spector, R. H. Singer, Dynamics of single mRNPs in nuclei of living cells. *Science* **304**, 1797–1800 (2004). Medline doi:10.1126/science.1099754

12. A. Mor, S. Suliman, R. Ben-Yishay, S. Yunger, Y. Brody, Y. Shav-Tal, Dynamics of single mRNP nucleocytoplasmic transport and export through the nuclear pore in living cells. *Nat. Cell Biol.* **12**, 543–552 (2010). Medline doi:10.1038/ncb2056

13. C. P. Stanners, The effect of cycloheximide on polyribosomes from hamster cells. *Biochem. Biophys. Res. Commun.* **24**, 758–764 (1966). Medline doi:10.1016/0006-291X(66)90390-1

14. T. Trcek, H. Sato, R. H. Singer, L. E. Maquat, Temporal and spatial characterization of nonsense-mediated mRNA decay. *Genes Dev.* **27**, 541–551 (2013). Medline doi:10.1101/gad.209635.112

15. J. R. Buchan, R. Parker, Eukaryotic stress granules: The ins and outs of translation. *Mol. Cell* **36**, 932–941 (2009). Medline doi:10.1016/j.molcel.2009.11.020

16. N. Kedersha, P. Ivanov, P. Anderson, Stress granules and cell signaling: More than just a passing phase? *Trends Biochem. Sci.* **38**, 494–506 (2013). Medline doi:10.1016/j.tibs.2013.07.004

17. N. Kedersha, G. Stoecklin, M. Ayodele, P. Yacono, J. Lykke-Andersen, M. J. Fritzler, D. Scheuner, R. J. Kaufman, D. E. Golan, P. Anderson, Stress granules and processing bodies are dynamically linked sites of mRNP remodeling. *J. Cell Biol.* **169**, 871–884 (2005). Medline doi:10.1083/jcb.200502088

18. S. Mollet, N. Cougot, A. Wilczynska, F. Dautry, M. Kress, E. Bertrand, D. Weil, Translationally repressed mRNA transiently cycles through stress granules during stress. *Mol. Biol. Cell* **19**, 4469–4479 (2008). Medline doi:10.1091/mbc.E08-05-0499

19. C. K. Damgaard, J. Lykke-Andersen, Translational coregulation of 5′TOP mRNAs by TIA-1 and TIAR. *Genes Dev.* **25**, 2057–2068 (2011). Medline doi:10.1101/gad.17355911

20. A. Ephrussi, R. Lehmann, Induction of germ cell formation by oskar. *Nature* **358**, 387–392 (1992). Medline doi:10.1038/358387a0

21. J. Kim-Ha, K. Kerr, P. M. Macdonald, Translational regulation of oskar mRNA by bruno, an ovarian RNA-binding protein, is essential. *Cell* **81**, 403–412 (1995). Medline doi:10.1016/0092-8674(95)90393-3

22. F. H. Markussen, A. M. Michon, W. Breitwieser, A. Ephrussi, Translational control of oskar generates short OSK, the isoform that induces pole plasma assembly. *Development* **121**, 3723–3732 (1995). Medline

23. E. Morais-de-Sá, A. Vega-Rioja, V. Trovisco, D. St Johnston, Oskar is targeted for degradation by the sequential action of Par-1, GSK-3, and the SCF¯Slimb ubiquitin ligase. *Dev. Cell* **26**, 303–314 (2013). Medline doi:10.1016/j.devcel.2013.06.011

24. M. D. Lin, X. Jiao, D. Grima, S. F. Newbury, M. Kiledjian, T. B. Chou, Drosophila processing bodies in oogenesis. *Dev. Biol.* **322**, 276–288 (2008). Medline doi:10.1016/j.ydbio.2008.07.033

25. D. Colak, S. J. Ji, B. T. Porse, S. R. Jaffrey, Regulation of axon guidance by compartmentalized nonsense-mediated mRNA decay. *Cell* **153**, 1252–1265 (2013). Medline doi:10.1016/j.cell.2013.04.056

26. C. Giorgi, G. W. Yeo, M. E. Stone, D. B. Katz, C. Burge, G. Turrigiano, M. J. Moore, The EJC factor eIF4AIII modulates synaptic strength and neuronal protein expression. *Cell* **130**, 179–191 (2007). Medline doi:10.1016/j.cell.2007.05.028

27. M. E. Tanenbaum, L. A. Gilbert, L. S. Qi, J. S. Weissman, R. D. Vale, A protein-tagging system for signal amplification in gene expression and fluorescence imaging. *Cell* **159**, 635–646 (2014). Medline doi:10.1016/j.cell.2014.09.039

28. M. Zuker, Mfold web server for nucleic acid folding and hybridization prediction. *Nucleic Acids Res.* **31**, 3406–3415 (2003). Medline doi:10.1093/nar/gkg595

29. J. A. Fitzpatrick, Q. Yan, J. J. Sieber, M. Dyba, U. Schwarz, C. Szent-Gyorgyi, C. A. Woolford, P. B. Berget, A. S. Waggoner, M. P. Bruchez, STED nanoscopy in living cells using Fluorogen Activating Proteins. *Bioconjug. Chem.* **20**, 1843–1847 (2009). Medline doi:10.1021/bc900249e

30. A. Coulon, M. L. Ferguson, V. de Turris, M. Palangat, C. C. Chow, D. R. Larson, Kinetic competition during the transcription cycle results in stochastic RNA processing. *eLife* **3**, e03939 (2014). Medline doi:10.7554/eLife.03939

31. D. R. Larson, C. Fritzsch, L. Sun, X. Meng, D. S. Lawrence, R. H. Singer, Direct observation of frequency modulated transcription in single cells using light activation. *eLife* **2**, e00750 (2013). Medline doi:10.7554/eLife.00750

32. B. Wu, J. A. Chao, R. H. Singer, Fluorescence fluctuation spectroscopy enables quantitative imaging of single mRNAs in living cells. *Biophys. J.* **102**, 2936–2944 (2012). Medline doi:10.1016/j.bpj.2012.05.017

33. T. Lionnet, K. Czaplinski, X. Darzacq, Y. Shav-Tal, A. L. Wells, J. A. Chao, H. Y. Park, V. de Turris, M. Lopez-Jones, R. H. Singer, A transgenic mouse for in vivo detection of endogenous labeled mRNA. *Nat. Methods* **8**, 165–170 (2011). Medline doi:10.1038/nmeth.1551

34. J. B. Grimm, B. P. English, J. Chen, J. P. Slaughter, Z. Zhang, A. Revyakin, R. Patel, J. J. Macklin, D. Normanno, R. H. Singer, T. Lionnet, L. D. Lavis, A general method to improve fluorophores for live-cell and single-molecule microscopy. *Nat. Methods* **12**, 244–250 (2015). 10.1038/nmeth.3256 Medline doi:10.1038/nmeth.3256

35. I. Weidenfeld, M. Gossen, R. Löw, D. Kentner, S. Berger, D. Görlich, D. Bartsch, H. Bujard, K. Schönig, Inducible expression of coding and inhibitory RNAs from retargetable genomic loci. *Nucleic Acids Res.* **37**, e50 (2009). Medline doi:10.1093/nar/gkp108

36. E. Bertrand, P. Chartrand, M. Schaefer, S. M. Shenoy, R. H. Singer, R. M. Long, Localization of ASH1 mRNA particles in living yeast. *Mol. Cell* **2**, 437–445 (1998). Medline doi:10.1016/S1097-2765(00)80143-4

37. N. F. Vanzo, A. Ephrussi, Oskar anchoring restricts pole plasm formation to the posterior of the Drosophila oocyte. *Development* **129**, 3705–3714 (2002). Medline